PERIODICA POLYTECHNICA SER. MECH. ENG. VOL. 48, NO. 2, PP. 119–132 (2004)

MECHANICAL PROPERTIES OF BASALT FIBRE REINFORCED PP/PA BLENDS

Jenő Sándor SZABÓ, Zoltán KOCSIS and Tibor CZIGÁNY

Department of Polymer Engineering
Budapest University of Technology and Economics
H–1521 Budapest, Műegyetem rkp.3., Hungary
Fax: +36 1 4631527
e-mail: czigany@eik.bme.hu

Received: July 8, 2004

Abstract

Short basalt fibre (BF) reinforced polypropylene/polyamide (PP/PA) blends were prepared by homogenization of the components in a twin-screw extruder followed by injection molding. In order to determine their static and dynamic mechanical properties tests have been performed on composites with different PA (0, 10, 20, 30, 40, and 50 wt%) and basalt fibre (0, 10, and 20 wt%) contents. Composite properties such as tensile and flexural strength, stiffness and fracture toughness have been calculated. It has been realized that the composite structure is very sensitive to the ratio of PA content. In case of small PA content (10–20 wt%), PA and basalt fibre have been experienced to form a kind of random network structure inside the PP matrix. This way could be improving the mechanical properties of the composite despite the relatively short fibre length. These results have been supported by acoustic emission (AE) tests and scanning electron (SEM) micrographs.

Keywords: hybrid composite, basalt fibre, acoustic emission.

1. Introduction

The compound systems having at least three components are called hybrid composites in which one or more different reinforcing or filling material is embedded in the matrix, which consists of one or more materials, in order to approach the desired mechanical and processing properties and to reduce costs of the base materials. The reinforced hybrid composites with polymer matrix (reinforced blends) possess several advantages and possibilities that were already studied and summarized by several authors in the literature [1]–[4].

Among the reinforced blends the PP/PA combination is especially significant and holds a lot of promises. This blend was used in our experiments considering the polarity property of the basalt fibre that allows the forming of an operating interface between the fibre and PA without any additives.

HARMIA and FRIEDRICH [5] examined the critical stress intensity factors (K_C) of long glass fibre reinforced PA66/PP hybrids in 75/25 and 25/75 weight percent PA66/PP systems and experienced that in the 25/75 case the value of K_C decreased significantly compared to the base polymer, while in the 75/25 case the result exceeded both initial values. Then 20 and 40 weight percent glass fibre

(GF) was added to the system. PP-g-MAL (PP-grafted-maleic anhydride) additive promoted adhesion and improved the contact between the two polymers and the reinforcing fibre. The most significant result of the study is that considering the critical stress intensity factor an almost isotropic material has been resulted in the 75/25/20 PA66/PP/LGF system in case of injection moulded specimens.

YU et al. [6] examined a PP/PA reinforcing system as well. The aim of their investigation was to study the effect of whisker used as reinforcement on the dielectric, static and dynamic properties. In this case PP-g-MAL additive was applied to associate the two polymers while the whisker was treated with two different silanes. The PP/PA weight ratio was constant (60/40). Their experience was that in case of 10–20% whisker content the crystals were only present in the PA phase, while in case of the 30–40% reinforcement content they also appeared in the PP phase. In the latter two cases the static and dynamic properties changed to a less extent than expected on the basis of increasing reinforcement content.

During our previous works [7, 8] it was found that the basalt fibre-like other well-known mineral fibres (ceramic, boron, asbestos etc.) – are very sensitive to the change of the processing parameters and the shear forces during processing (the fibre is very brittle) and the fibre/fibre interaction is also significant [9]. In order to avoid these effects PA was added to the PP matrix to improve the fibre/matrix interfacial connection [6] and hence improve the mechanical properties and to reduce fibre breakage caused by the shear forces during processing. In order to improve the PP/PA connection PP-g-MAL was added to the polymer.

The aim of the paper is to develop a basalt fibre reinforced composite structural material that can be injection-moulded, using the polar and apolar properties [10] of the materials (PP/PA/fibre) and to reveal the characteristic failure modes in case of the basalt fibre reinforced PP/PA blend.

2. Experimental

2.1. Materials

The base matrix was PP homopolymer (TVK H116F, Hungary) developed exactly for extrusion and hence having very good flowability ($MFI_{230\ ^\circ C/2.16\ kg} = 25$ g/10 min). The other base material of the hybrid matrix was PA12 (UBESTA 3030 JFX 1, Japan), the melt flow index of which is $MFI_{230\ ^\circ C/2.16\ kg} = 7.4$ g/10 min. The ratio of PA in the blend was 0, 10, 20, 30, 40 and 50 weight percent. In order to ensure the interfacial adhesion between the two base polymers 5 phr PP-g-MAL (SCONA® TPPP 2112 FPA, KOMETRA, Germany) was used. 4–8 mm long, chopped short basalt fibres of 6–11 μm diameter were used as reinforcing material. The components of basalt fibres were SiO_2 – 46.2%; Al_2O_3 – 13.0%; $Fe_2O_3 + TiO_2$ – 14.0%; $MgO + CaO$ – 20.0%; $Na_2O + K_2O$ – 5.3% and others $\leq$ 1.5 wt%.

2.2. Production of Composites and Specimens

In the first step the PP/PA blend was prepared in the adequate ratio and a sufficient amount of PP-g-MAL was added. Then the material that was going to be the material of the matrix was homogenized in a BRABENDER type twin-screw extruder (Plasticorder PL2100) with the following parameters set: zone temperatures: 185–190–195–200 °C and the velocity of the screws: 20 rpm (as suggested by the producer of the PP-g-MAL). Then the fibres were added to the matrix during another extrusion. The processing parameters were adjusted to the parameters of the forthcoming injection moulding and processing was carried out at the relevant temperatures while the velocity of the screw remained constant. Injection moulding was completed on an injection moulding machine type ARBURG 270 C. Zone temperatures were 170–175–180–185–190 °C, injection pressure was 1350 bar and the pressure holding 1100 bar, while the temperature of the mould changed between 35 and 40 °C. Standard dumbbell specimens were produced considering the recommendations of the standard (ISO 3167 A). Five specimens of each type were tested and then the best and worst results were neglected. Hence, the mean value was calculated from three pieces of data in each case.

2.3. Static Mechanical Tests

Tensile Test

The determination of the tensile strength of composites was carried out according to the recommendation of standard ASTM D 3039. The most important dimensions of the specimen were: 4 mm thickness, 10 mm width and 100 mm operating length. The experiments were completed on a universal loading machine type INSTRON 5566 at the velocity of 2 mm/min at room temperature.

Flexural Test

The bending strength of the composite was determined in a three-point bending test on the basis of the recommendations of standard ASTM D 790–02. The dimensions of the specimen were $4 \times 10 \times 80$ mm^3 and the span length was 64 mm. The experiments were carried out on a universal tensile tester type ZWICK Z020 at the velocity of 2 mm/min at room temperature.

Measurement of the Stress Intensity Factor on SEN-T Specimens

K_C was calculated based on the ESIS protocol [11]. Notched dumbbell specimens were used in the experiments. The notch was created with a diamond-coated saw

and sharpened by a blade so that the crack front could be well traced. The size of the notch was ca. 2 mm. The experiments were carried out on a universal tensile tester type ZWICK Z020 at the velocity of 2 mm/min at room temperature.

2.4. Dynamic Mechanical Tests

Charpy-Test

Specimens were cut from the injection-moulded parts ($4 \times 10 \times 80$ mm^3, span length 62 mm) for these tests considering the recommendations of standard ASTM D 5942. The notching and cutting altogether changed between 1.55 and 3.30 mm. The experiments were carried out on an instrumented impact-tester type CEAST-DAS 8000. The impact energy was 2 J and the impact velocity was 2.9 m/s.

2.5. Failure Characterization

The failure after tests were studied with the help of a scanning electron microscope (SEM; Jeol JSM 54000). Prior to the SEM investigations, the fracture surfaces were coated with Au/Pd alloy in a Balzers SCD 050 device to evade electrostatic charging.

During loading the SEN-T specimens, acoustic emission (AE) was monitored by a microprocessor-controlled AE device (Defectophone NEZ-220, Atomic Energy Research Institute, Budapest, Hungary). The acoustic events were picked up with transducer (type: DAE – 002P IN – T ELEKTROSVARKI IM.E.O. PATONA, Russia). The output signal of the transducer was amplified logarithmically. During the tests the elapsed time, the number of events, and the peak amplitude were measured, calculated and stored.

3. Results and Discussion

3.1. Static Tension Response

The results of the experiment can be found in *Table 1*. It can be claimed that in case of the pure PP matrix the strength decreases when the basalt content increases. This leads to a conclusion that during processing fibres break into pieces shorter than the critical length, hence they are present as a filling material in the composite. On the contrary, when PA was added to the matrix this effect changed and the strength of the composite increased significantly. A better material is expected to form if the PA content increases but – as it can be seen in *Table 1* as well – this does not happen. It can also be clearly seen that in case of composites with small PA content

the change of the ratio of basalt altered the strength to a great extent, while this process is negligible in case of higher PA content.

Table 1. Tensile mechanical characteristics of the PP/PA hybrid combinations with and without basalt fibre reinforcement.

PP/PA hybrid	Matrix	Composite (fibre content)	
		10 wt%	20 wt%
		E-modulus [GPa]	
100/ 0	1.27 ± 0.03	1.76 ± 0.10	2.21 ± 0.30
90/10	1.42 ± 0.06	1.88 ± 0.05	2.61 ± 0.08
80/20	1.47 ± 0.06	1.90 ± 0.06	2.45 ± 0.07
70/30	1.21 ± 0.05	1.72 ± 0.09	2.04 ± 0.14
60/40	1.10 ± 0.06	1.56 ± 0.07	1.92 ± 0.03
50/50	0.99 ± 0.05	1.33 ± 0.03	1.85 ± 0.12
		Strength [MPa]	
100/ 0	26.51 ± 0.54	25.10 ± 0.02	24.89 ± 0.10
90/10	28.89 ± 0.38	29.78 ± 0.25	30.70 ± 0.20
80/20	29.66 ± 0.62	30.01 ± 0.68	30.41 ± 0.39
70/30	27.42 ± 0.12	28.67 ± 0.58	28.74 ± 0.17
60/40	26.56 ± 0.14	28.20 ± 0.42	28.24 ± 0.08
50/50	26.38 ± 0.27	26.54 ± 0.10	26.70 ± 0.13
		Elongation [%]	
100/ 0	10.41 ± 0.51	9.26 ± 0.06	7.46 ± 0.56
90/10	9.48 ± 0.06	6.72 ± 0.47	4.71 ± 0.12
80/20	10.93 ± 0.35	7.60 ± 0.08	5.67 ± 0.19
70/30	12.92 ± 0.09	9.73 ± 0.22	8.45 ± 0.61
60/40	15.79 ± 0.69	12.81 ± 0.11	10.01 ± 0.35
50/50	18.08 ± 0.74	10.65 ± 0.87	9.54 ± 0.76
		K_c [MPam$^{1/2}$]	
100/ 0	2.44 ± 0.12	2.42 ± 0.12	2.24 ± 0.14
90/10	1.46 ± 0.12	2.50 ± 0.20	2.65 ± 0.16
80/20	1.53 ± 0.08	2.68 ± 0.23	2.79 ± 0.52
70/30	1.69 ± 0.07	2.52 ± 0.06	2.51 ± 0.21
60/40	1.72 ± 0.17	2.45 ± 0.18	2.26 ± 0.07
50/50	1.75 ± 0.08	2.44 ± 0.13	2.19 ± 0.24

3.2. Static Flexural Response

Table 2 contains the results of the three-point bending test that shows the same tendency as the tensile test results but the presence of basalt fibre leads to a remarkable increase in strength in all composites. The results show that the composite with basalt fibre can bear more bending load and this characteristic is highlighted even more by the presence of PA.

Table 2. Flexural mechanical characteristics of the PP/PA hybrid combinations with and without basalt fibre reinforcement.

PP/PA hybrid	Matrix	Composite (fibre content)	
		10 wt%	20 wt%
	E-modulus [GPa]		
100/ 0	1.67 ± 0.04	2.50 ± 0.05	2.90 ± 0.12
90/10	1.89 ± 0.03	2.52 ± 0.08	3.15 ± 0.09
80/20	2.06 ± 0.05	2.65 ± 0.03	3.15 ± 0.10
70/30	1.64 ± 0.02	2.52 ± 0.07	2.84 ± 0.08
60/40	1.63 ± 0.07	2.18 ± 0.09	2.54 ± 0.11
50/50	1.55 ± 0.03	2.02 ± 0.06	2.52 ± 0.08
	Strength [MPa]		
100/ 0	48.72 ± 0.14	51.85 ± 0.49	53.27 ± 0.37
90/10	53.49 ± 0.17	63.05 ± 0.36	64.34 ± 0.52
80/20	61.09 ± 0.64	62.79 ± 1.46	64.67 ± 0.14
70/30	51.79 ± 1.06	57.13 ± 1.43	59.87 ± 0.38
60/40	47.77 ± 1.28	53.65 ± 0.59	57.01 ± 0.53
50/50	46.21 ± 1.17	50.59 ± 0.26	54.27 ± 0.42
	Elongation [%]		
100/ 0	8.87 ± 0.20	7.99 ± 0.41	7.41 ± 0.03
90/10	8.60 ± 0.15	7.31 ± 0.12	5.93 ± 0.25
80/20	9.02 ± 0.24	7.45 ± 0.48	6.07 ± 0.03
70/30	9.31 ± 0.39	7.67 ± 0.44	7.19 ± 0.20
60/40	9.59 ± 0.60	9.05 ± 0.21	8.20 ± 0.10
50/50	8.92 ± 0.12	8.12 ± 0.37	7.58 ± 0.12

Table 3. Dynamic mechanical characteristics of the PP/PA hybrid combinations with and without basalt fibre reinforcement.

PP/PA hybrid	Matrix	Composite (fibre content)	
		10 wt%	20 wt%
		E-modulus [GPa]	
100/ 0	1.09 ± 0.04	1.14 ± 0.11	1.33 ± 0.06
90/10	0.90 ± 0.02	1.94 ± 0.20	2.37 ± 0.19
80/20	0.84 ± 0.06	1.59 ± 0.10	1.73 ± 0.10
70/30	0.73 ± 0.03	1.16 ± 0.09	1.54 ± 0.10
60/40	0.64 ± 0.02	1.15 ± 0.08	1.42 ± 0.15
50/50	0.61 ± 0.05	0.79 ± 0.08	1.12 ± 0.06
		Strength [MPa]	
100/ 0	97.30 ± 0.24	94.92 ± 0.98	95.39 ± 1.12
90/10	95.60 ± 0.47	96.57 ± 2.34	105.83 ± 1.71
80/20	96.65 ± 0.65	98.46 ± 1.99	107.05 ± 0.88
70/30	84.72 ± 1.89	95.89 ± 2.07	97.39 ± 1.82
60/40	79.53 ± 0.57	93.69 ± 0.95	95.19 ± 1.98
50/50	78.25 ± 0.48	85.06 ± 1.10	86.92 ± 0.87
		K_D [MPam$^{1/2}$]	
100/ 0	2.59 ± 0.22	3.53 ± 0.18	4.17 ± 0.21
90/10	3.22 ± 0.11	3.71 ± 0.10	4.33 ± 0.25
80/20	3.83 ± 0.13	3.89 ± 0.33	4.54 ± 0.20
70/30	3.62 ± 0.15	3.88 ± 0.42	4.35 ± 0.10
60/40	2.95 ± 0.45	3.70 ± 0.04	3.75 ± 0.38
50/50	2.85 ± 0.19	3.65 ± 0.16	3.70 ± 0.22

3.3. Dynamic Response

On the basis of results (*Table 3*) it was found that a small amount of PA content increases impact strength, while a greater amount has no significant effect. Results also show well that our preliminary assumption – according to which basalt fibres have only a filling role in the matrix – was right since the dynamic strength improved as expected [12]–[13].

Examining the results of the dynamic tests the effect of the differences in the test velocity, the loading modes etc. can again be claimed. It can be seen clearly that the effect of increasing fibre content – due to the good resistance of basalt fibres

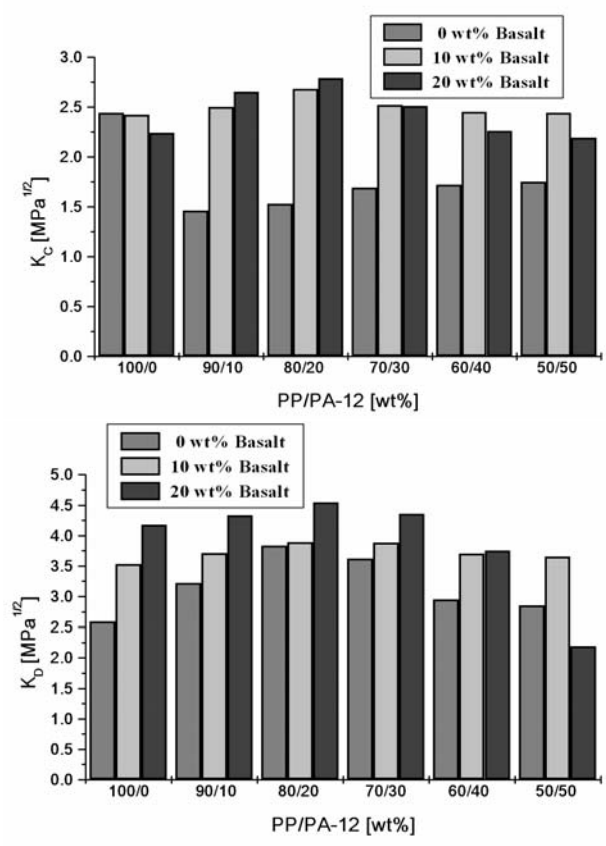

Fig. 1. Critical fracture toughness of basalt fibre reinforced PP/PA blends, static (a); dynamic (b).

to pressure – is advantageous in this case as well. Significant improvement can be detected especially in case of the 20 % reinforcement content and composites with smaller PA content.

3.4. Failure Behaviour

The values of the critical stress intensity factor determined in static tests do not show uniform behaviour. The tendencies partly turn around in case of high PA content. The results of composites with low PA content are more favourable in this case as well. It can be seen that the effect of PA in case of fibre reinforcement is not remarkable; in fact it is within the deviation. *Fig. 1* shows that the fibre content

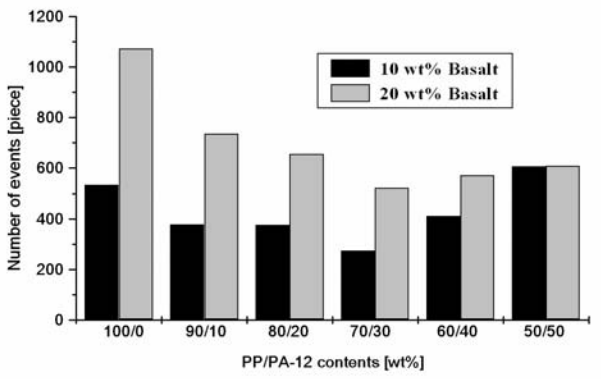

Fig. 2. Cummulative number of events in basalt fibre reinforced PP/PA blends.

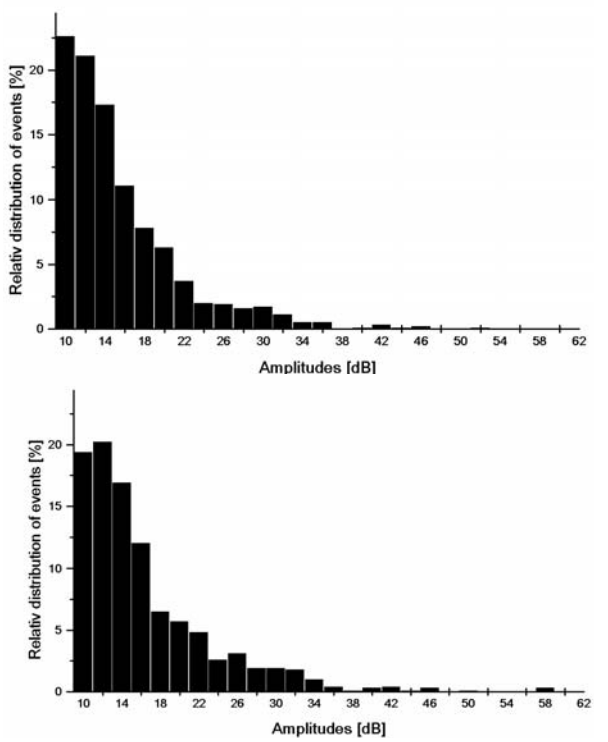

Fig. 3. Distribution of the AE amplitudes up to F_{max} in basalt fibre reinforced PP/PA blends; at 0 wt% PA and 20 wt% basalt fibre (a); – at 30 wt% PA and 20 wt% basalt fibre (b).

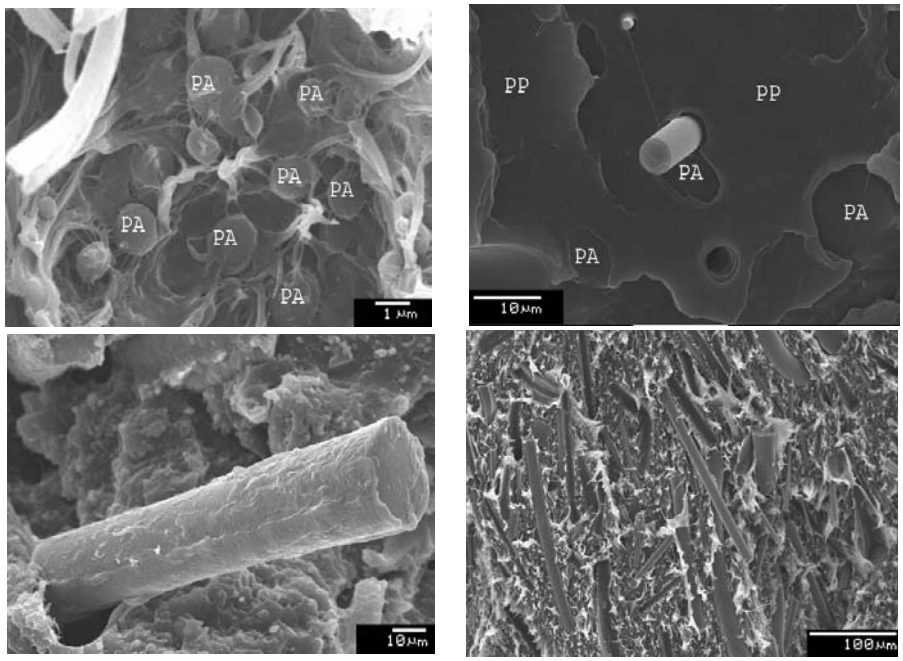

Fig. 4. SEM pictures taken of the fracture surface of SEN-T specimens cut out from the basalt fibre reinforced PP/PA matrix composites with and without fibres type 40 wt% PA (a), 10 wt% PA and 10 wt% fibre (b) 40 wt% PA and 20 wt% fibre (c), and 50 wt% PA and 20 wt% fibre (d).

influences the values of the critical stress intensity factor considerably both in case of static (*Fig. 1a*) and dynamic (*Fig. 1b*) loading.

After the AE results have been analysed it can be claimed that if the reinforcement content increases, the number of events increases as well in case of composites with the same matrix [14]. When the PA content increases, the change is not so unambiguous but it seems to support the tendency of strength results and the conclusions that can be drawn from them. *Fig. 2* shows the number of detected events as a function of PA and basalt content. The most events can be seen in case of composites with 100% PP content both in case of composites with 10% and 20% basalt content, while the fewest events were detected in case of composites with 30% PA content. The results show well that when fibres separate or pull out from PP there are more events when failure occurs concerning PA/basalt. In case of the 30% PA content a few events are resulted by the PP/PA interfacial separation, which involves great plastic deformation, hence does not induce acoustic signals, as an opposite to fibre/matrix failure where friction induces a large number of events.

If the distribution of amplitudes is studied (*Fig. 3a–3b*), it is obvious that most

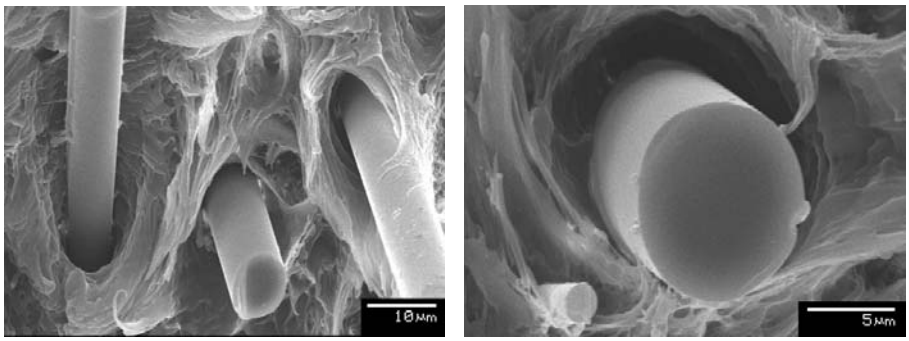

Fig. 5. SEM pictures taken of the fracture surface of SEN-T specimens cut out from the basalt fibre reinforced PP/PA matrix composites type 30 wt% PA and 20 wt% fibre with fibres after acid treatment – xylol treated (a), 30 wt% PA and 20 wt% fibre – formic acid treated (b).

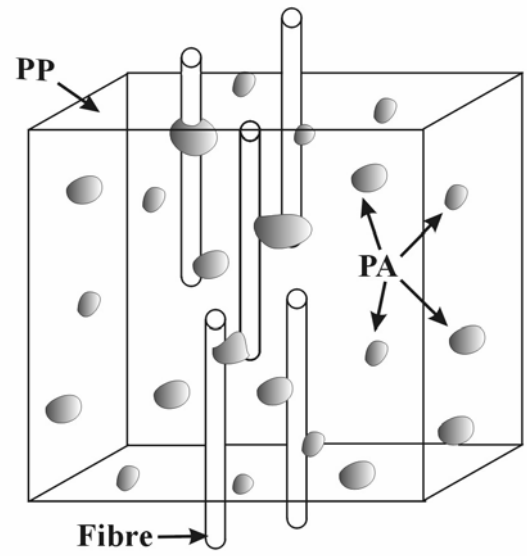

Fig. 6. Scheme of the co-continuous phase structure in a PP/PA/basalt fibre system

events are between 10 and 40 dB, while the maximum is below 60 dB. Analysing the pure PP matrix composites and comparing them to our previous results [12], the failure turns out to be definitely matrix deformation and matrix tearing, while the higher signals refer to debonding and fibre pull-out. The value of the maximal amplitude did not increase as a result of PA content as an opposite to what was expected. Hence it can be found that due to the PA content a kind of damped

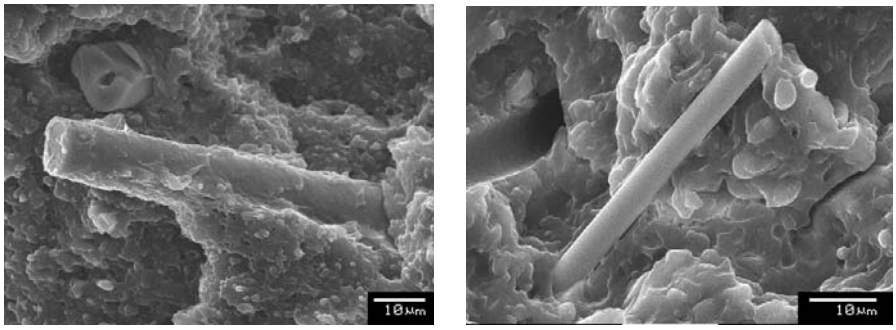

Fig. 7. SEM pictures taken of the fracture surface of SEN-T specimens cut out from the basalt fibre reinforced PP/PA matrix composites of type 50 wt% PA and 20 wt% fibre with fibres after acid treatment – formic acid treated (a), 50 wt% PA and 20 wt% fibre – xylol treated (b).

mechanical system is created what results in noise damping within the system and leads to the amplitude distribution shown in *Fig.3a–3b*. The plastic, highly flexible PP/PA interfacial connection shown in *Fig.4a* refers to the damped system, the result of which is the lack of the acoustic activity of the matrices. Debonding between the two polymers, if the connection is not even established or is very weak, results in an acoustically active interfacial connection that was not detected in this case.

On the basis of SEM images in *Fig. 4* some of our preliminary assumptions can be verified:

1. *Fig. 4a* shows that PA is present in a homogeneous form and in small size (that is why it increases the strength) in composites with small PA content.
2. *Fig. 4b* reveals why the mechanical properties of composites with low PA content improved. The figure shows that PA is connected to the fibre but since it is present only in a small amount this connection is established only in a few places along the length of the fibre. This structure results in an elastic composite proven by the improved dynamic properties and the fact that the elasticity of the composite did not change in the presence of fibers in opposite to other composites.
3. *Figs. 4c–4d* show why most mechanical properties do not improve further if PA content increases. On the basis of the images and examination results it was concluded that PA forms a continuous shield around the fibre and the contact surface between the two polymers is specifically smaller because of a larger co-continuous system. As a consequence in case of 30–40 wt% PA content the fibre can tear out from the matrix along the weaker PP/PA surface as it can be seen in *Fig. 4c*. If the PA content is very high the role of phases can even be changed within the matrix (phase inversion). In this case the main matrix will be PA, hence the relatively longer fibres tear out from the PP phase.

In order to verify the preliminary assumptions the surface was etched with formic acid and xylol since the former is a well-known solvent of PA and xylol is of PP. The image (*Fig. 5a*) is taken after the partial soluting of the PP phase in the composite with lower PA content. The partial presence of the fibre/matrix connection can be seen well while after dissolving PA (*Fig. 5b*) only the place of PA dissolved from near the fibre, the lack of the phase along the fibre can be found. The basalt fibre/PA/PP connection and the co-continuous phase structure created by the PA/basalt fibre are modelled in *Fig. 6*.

A continuous PA phase can be found on the surface of fibres (*Fig. 7a*) at higher PA content after etching with xylol. In case of the formic acid etching (*Fig. 7b*) the fibre stayed free and PP spheres can be noticed around it that do not create a continuous phase as opposed to composites of low PA content.

4. Conclusion

Short basalt fibre reinforced PP/PA blends were examined from the point of view of revealing the effect of the amount of PA on the mechanical properties. The following statements can be made after analysing the results:

1. During processing the fibres break to a great extent because of the fibre/fibre interaction, hence much shorter fibres are obtained than the critical fibre length. These fibres play a filling role in the composite and this way they reduce the static mechanical properties and increase the dynamic ones.
2. PA improves the mechanical properties of composites if it is present only in a small amount and this is in connection with the good fibre/PA interaction according to our assumptions. In case of adequate homogeneity and spatial distribution, a kind of co-continuous structure is realized and this is responsible for the noticed change in properties.
3. In case of higher PA content PA embeds the fibres and the smaller interaction of the PA/PP interfacial layer causes the less favourable properties and a dual-phase system is formed until a 50/50 wt% phase inversion can be created.

Acknowledgements

This work was supported by the Hungarian Ministry of Education (NKFP 3/001/2001).

We thank the Norco Hungaria Ltd. and Kometra for material support.

References

[1] KARGER-KOCSIS, J., Reinforced Polymer Blends, Polymer Blends, Vol.2: Performance, Edited by DR. Paul and CB. Bucknall (2000) Ch.31. pp. 395–428.

[2] TJONG, S. C. – MENG, Y. Z., Properties and Morphology of Polyamide 6 Hybrid Composites Containing Potassium Titanate Whisker and Liquid Crystalline Copolyester, *Polymer*, **40** (1999), pp. 1109–1117.
[3] OKADA, O. – KESKKULA, H. – PAUL, D. R., Fracture Toughness of Nylon 6 Blends with Maleated Ethylene/Propylene Rubbers, *Polymer*, **41** (2000), pp. 8061–8074.
[4] LAURA, D. M. – KESKKULA, H. – BARLOW, J. W. – PAUL, D. R., Effect of Glass Fiber Surface Chemistry Ont the Mechanical Properties of Glass Fiber Reinforced, Rubber-Toughened Nylon 6, *Polymer*, **43** (2002), pp. 4673–4687.
[5] HARMIA, T. – FRIEDRICH, K., Fracture Toughness and Failure Mechanisms in Unreinforced and Long-Glass-Fiber-Reinforced PA66/PP Blends, *Compos. Sci. Technol.*, **53** (1995), pp. 423–430.
[6] YU, D. – WU, J. – ZHOU, L. – XIE, D. – WU, S., The Dielectric and Mechanical Properties of a Potassium-Titanate-Whisker-Reinforced PP/PA Blend, *Compos. Sci. Technol.*, **60** (2000), pp. 499–508.
[7] SZABÓ, J. S. – CZIGÁNY, T., Investigation of Static and Dynamic Fracture Toughness on Short Ceramic Fiber Reinforced Polypropylene Composites, *J. Macromol. Sci. Phys.*, **B41** (2002), pp. 1191–1204.
[8] SZABÓ, J. S. – CZIGÁNY, T., Static Fracture and Failure Behaviour of Aligned Discontinuous Mineral Fiber Reinforced Polypropylene Composites, *Polym. Test.*, **22** (2003), pp. 711–719.
[9] FU, S. Y. – MAI, Y. W. – LAUKE, B. – YUE, C. Y., Synergistic Effect on the Fracture Toughness of Hybrid Short Glass Fiber Reinforced Polypropylene Composites, *Mat. Sci. Eng. A*, *323* (2002), pp. 326–335.
[10] CZVIKOVSZKY, T. – HARGITAI, H. – RÁCZ, I. – CSUKAT, G., Reactive Compatibilization in Polymer Alloys, Recyclates and Composites, *Nucl. Instr. and Meth. B*, **151** (1999), pp. 190–195.
[11] WILLIAMS, J. G., K_c and G_c at Slow Speed for Polymers, In: D. R. Moore, A. Pavan, J. G. Williams editors. *Fracture Mechanics Testing Methods for Polymers Adhesives and Composites – ESIS 28*, Oxford: Elsevier Sci. (2001), pp. 11–26.
[12] KARGER–KOCSIS, J., Instrumented Impact Fracture and Related Failure Behavior in Short- and Long-Glass-Fiber-Reinforced Polypropylene, *Compos. Sci. Technol.*, **48** (1993), pp. 273–283.
[13] MOLNÁR, SZ. – PUKÁNSZKY, B. – HAMMER, C. O. – MAURER, F. H. J., Impact Fracture Study of Multicomponent Polypropylene Composites, *Polymer*, **41** (2000), pp. 1529–1539.
[14] CZIGÁNY, T. – KARGER–KOCSIS, J., Comparison of the Failure Mode in Short and Long Glass-Fiber-Reinforced Injection-Moulded Polypropylene Composites by Acoustic-Emission, *Polym. Bull.*, **31** (1993), pp. 495–501.